HHS Public Access

Author manuscript

Nat Protoc. Author manuscript; available in PMC 2016 July 11.

Published in final edited form as:

Nat Protoc. ; 6(11): 1683–1694. doi:10.1038/nprot.2011.373.

Selective 2′-Hydroxyl Acylation analyzed by Protection from Exoribonuclease (RNase-detected SHAPE): direct analysis of covalent adducts and of nucleotide flexibility in RNA

Kady-Ann Steen, **Nathan A. Siegfried**, and **Kevin M. Weeks**

Department of Chemistry, University of North Carolina, Chapel Hill, NC 27599-3290

Abstract

RNA SHAPE chemistry yields quantitative, single nucleotide resolution structural information based on the reaction of the 2′-hydroxyl group of conformationally flexible nucleotides with electrophilic SHAPE reagents. However, SHAPE technology has been limited by the requirement that sites of RNA modification be detected by primer extension. Primer extension results in loss of information at both the 5′ and 3′ ends of an RNA and requires multiple experimental steps. Here we describe RNase-detected SHAPE (Selective 2′-Hydroxyl Acylation analyzed by Protection from Exoribonuclease) that uses a processive, 3′→5′ exoribonuclease, RNase R, to detect covalent adducts in 5′-end labeled RNA in a one-tube experiment. RNase R degrades RNA but stops quantitatively three and four nucleotides 3′ of a nucleotide containing a covalent adduct at the ribose 2′-hydroxyl or the pairing face of a nucleobase, respectively. We illustrate this technology by characterizing ligand-induced folding for the *E. coli* thiamine pyrophosphate riboswitch RNA. RNase-detected SHAPE is a facile, two-day approach that can be used to analyze diverse covalent adducts in any RNA molecule, including short RNAs not amenable to analysis by primer extension and RNAs with functionally important structures at their 5′ or 3′ ends.

Keywords

Selective 2′-Hydroxyl Acylation analyzed by Primer Extension; chemical probing; RNA structure prediction; covalent adducts; RNase R

INTRODUCTION

Most RNA molecules form specific secondary and tertiary structures as a prerequisite for carrying out their function[1,2]. Moreover, both large-scale and subtle conformational changes impact the biological roles of many RNAs. Chemical probing technologies have proven to be especially powerful for understanding both global and fine-scale components of RNA

Correspondence should be addressed to K.M.W. (weeks@unc.edu).

SUPPORTING INFORMATION

Protocols for affinity purification of the *M. genitalium* RNase R enzyme and for synthesis of the 1M7 reagent, plus a sample dataset corresponding to the experiment shown in Figure 3.

Author Contributions: K.-A. S. and K.M.W. collaborated on all aspects of the conception and writing of this paper. N.A.S. and K.M.W. wrote the Supporting Protocol on RNase R purification.

Competing Financial Interests: The authors declare no competing interests.

structure[3,4]. Selective 2′-Hydroxyl Acylation analyzed by Primer Extension (SHAPE) yields quantitative and nucleotide-resolution structural information for RNAs ranging in size from tRNA and small riboswitches[5,6] to entire RNA genomes[7,8]. SHAPE chemistry takes advantage of the discovery that the reactivity of the 2′-hydroxyl position is highly sensitive to the precise conformation of a given nucleotide. Flexible nucleotides adopt many different conformations, a subset of which increases the nucleophilicity of the 2′-hydroxyl group. Electrophilic SHAPE reagents thus react preferentially at dynamic or conformationally flexible nucleotides to form 2′-*O*-adducts. Constrained nucleotides sample fewer conformations and generally show low reactivity with SHAPE reagents (Figure 1a)[5,9].

Using this simple chemical modification reaction, it is possible to obtain a comprehensive view of RNA structure because most RNA nucleotides have a free 2′-hydroxyl, all four nucleotides react similarly with SHAPE reagents[10], and reactivities correlate closely with biophysical measurements of local order in RNA[11]. All SHAPE reagents undergo an auto-inactivating hydrolysis reaction with water (Figure 1b)[9,12]; this self-quenching reaction (with 55 M water) is so dominant that SHAPE chemistry is insensitive to the presence of most common biological buffer components. Thus, SHAPE chemical probing reactions can be performed in the presence of proteins, ligands, and other RNAs[6,13–15] and in complex biological environments including inside viruses[7,16]. SHAPE reactivity data can be used to inform structure prediction algorithms to generate highly accurate RNA secondary structure models[17].

Primer extension was first used to detect RNA cleavage fragments and covalent adducts resulting from chemical probing experiments over 20 years ago[18,19]. In primer extension, reverse transcriptase enzymes synthesize cDNA from an RNA template. Extension is inhibited when an RNA strand has been cleaved or the RNA base or backbone has been modified such that base pairing ability is disrupted. Extension is also inhibited if the adduct becomes too large to be accommodated in the polymerase active site. Primer extension coupled with recent innovations, including the use of fluorescently labeled DNA primers, analysis by automated capillary electrophoresis, availability of highly processive polymerases, and automated quantification of reactivity patterns, now makes it possible to obtain single-nucleotide resolution structural information for 300–650 nucleotides in a single experiment[4,20,21]. Thus, primer extension is the technology of choice when long read lengths are the primary consideration.

However, detection of RNA adducts by primer extension has important limitations and results in some regions of an RNA being inaccessible to analysis. First, reverse transcriptase-mediated primer extension requires that a DNA oligonucleotide bind at a specific site 3′ to the region of interest. Second, the imperfect processivity of reverse transcriptase during the initial stage of primer extension results in pausing adjacent to the primer binding site. These factors result in a loss of structural data for 40–60 nucleotides at the 3′ end of the RNA. Third, primer extension typically results in a large number of cDNAs that correspond to full-length extension products. These full-length products overlap with and result in a loss of structural data for 5–20 nucleotides at the 5′ end of the RNA. The combined loss of 45–80 nucleotides of data at the 5′ and 3′ ends makes structural analysis of short RNAs in their native forms essentially impossible. The limitations of primer extension-based structure

probing are also evident in longer RNA sequences where structural data is not obtained at the ends[8,17]. A useful solution to this problem involves appending non-native flanking sequences, a “structure cassette”, on both ends of the RNA to move the region of interest to the readable center of the RNA[22]. Finally, although powerful and highly quantitative, the primer extension process requires multiple biochemical manipulations, RNA-specific primer design, and optimization of annealing and extension conditions.

RNase-detected SHAPE addresses these limitations by using a processive, nonspecific, 3′→5′ exoribonuclease from *Mycoplasma genitalium* (RNase R) to detect covalent adducts in RNA[6]. RNase-detected SHAPE makes possible the direct analysis of RNA fragments that have been chemically modified either by SHAPE reagents that react at the ribose 2′-hydroxyl group or reagents that react at the base pairing face of nucleobases[6]. The *M. genitalium* RNase R enzyme belongs to the ubiquitous RNR family of exoribonucleases that hydrolytically degrade structured RNAs to release 5′-monophosphates without requiring an exogenous helicase[23–25].

Although a high-resolution structure of the *M. genitalium* RNase R enzyme is not currently available, we can make structural inferences based on homology modeling using the *E. coli* RNase II[26] and *S. cerevisiae* Rrp44[27] structures. The RNase R enzyme consists of four major domains: two N-terminal cold shock domains, CSD1 and CSD2; a central, highly conserved, ribonuclease (RNB) domain; and a C-terminal S1 domain (Figure 2). The RNB domain contains the RNA substrate-binding channel and the active site for hydrolytic degradation of RNA (Figure 2, inset). The RNA strand is threaded to the RNB domain through an opening between the CSD1 and RNB domains (Figure 2, black strand) and makes numerous contacts with protein residues in the RNB domain (Figure 2, inset).

Experimentally, we discovered that RNA fragments containing 2′-*O*-adducts or modifications at the base-pairing face of guanosine are 3 and 4 nucleotides longer, respectively, than the actual site of modification[6]. These fragment lengths were determined by comparison with guanosine markers generated by iodine-mediated cleavage of the phosphorothioate-substituted backbone in adduct-free RNAs[6]. The offsets are due to the different contacts made by the 2′-hydroxyl group and the nucleotide base-pairing face of the RNA within the substrate binding channel of the RNase R enzyme. RNase R glutamic acid residue 463 forms a hydrogen bond with the 2′-hydroxyl group of nucleotide N-3 (Figure 2, red sphere). In contrast, serine 433 makes a hydrogen bond at nucleotide N-4 (Figure 2, blue nucleotide). This “two site” model for interactions between the enzyme and the RNA strand is supported by two pieces of data. First, glutamic acid at position 463 is evolutionarily conserved throughout the RNR enzyme family and interacts with the 2′-hydroxyl of RNA in several family members[26,27]. Mutation of this residue in RNase II from glutamic acid to alanine results in a loss of RNA cleavage specificity[28]. Second, although the residue is not always a serine, a hydrogen bonding interaction between a residue in the substrate channel and the nucleotide base-pairing face at N-4 is also highly conserved.

RNase-detected SHAPE was previously used to characterize structural transitions induced upon ligand binding to the aptamer domain of the *Escherichia coli* thiamine pyrophosphate (TPP) riboswitch[6]. RNase-detected SHAPE analysis of the TPP riboswitch revealed the

secondary structure of the ligand-free state, the nucleotides undergoing the largest conformational changes upon ligand binding, and the existence of a single nucleotide bulge register shift that likely modulates a long-range tertiary interaction. The usefulness of RNase-detected SHAPE is general and we anticipate that this approach will make possible structural analysis of miRNAs and their precursors, riboswitches, and small non-coding RNAs in their native forms. RNase-detected SHAPE will also facilitate complete analysis of functionally important structures at the 5′ and 3′ ends of large RNAs, including the genomes of RNA viruses.

EXPERIMENTAL DESIGN

RNase-detected SHAPE yields quantitative reactivity data for almost every position in an RNA. The technology combines the previously well-characterized SHAPE acylation reaction[9,12,29] with a simple 3′→5′ enzymatic degradation step using a 5′-end labeled RNA. The current protocol is optimized for highly structured short RNAs (approximately 80–140 nucleotides). However, RNase R digestion temperature and time can be optimized for analysis of longer RNAs. The key experimental variable is that RNase R enzyme activity is strongly sensitive to Mg^{2+} concentration. The optimal range of Mg^{2+} concentration for RNase R activity with structured RNAs is 0.25 – 0.50 mM. All nucleotide positions up to and including the 3′ end can be resolved with sufficiently long electrophoresis times. Information for approximately five nucleotides at the 5′-end of the RNA is obscured because, at the end of digestion, the RNase R enzyme remains bound to the very end of the RNA strand.

RNAs and RNA folding

RNase-detected SHAPE is ideally suited for analysis of short *in vitro* transcripts. This protocol highlights analysis of changes in conformational states that occur upon small molecule binding to a riboswitch RNA and uses an RNA folding approach and buffer conditions that work well for the TPP riboswitch RNA. Other RNAs may require different conditions: essentially any folding environment appropriate for an RNA of interest can be used. RNase-detected SHAPE can be applied to understanding the changes in RNA folding as a function of temperature, ion concentration, and in the presence of proteins or ligands. The RNA of interest must be 5′-end labeled[30,31] to facilitate detection of RNase digestion products by electrophoretic separation.

RNA modification

Any SHAPE reagent[9,12,29,32] can be used in RNase-detected SHAPE (for a summary of useful reagents, see Ref. 33). For this protocol, we used 1-methyl-7-nitroisatoic anhydride (1M7)[12]. However, any reagent that reacts with an RNA nucleotide and is sufficiently bulky to inhibit movement of the RNA within the RNase R active site (Figure 2) is detectable by this approach. For SHAPE electrophiles, the reagent is added to the folded RNA and allowed to react until inactivation by hydrolysis is complete (Figure 1). SHAPE reagents thus do not require an explicit quench step. For most conventional reagents, a quench step is required; for example, kethoxal is quenched with unbuffered boric acid[18]. In addition, a no reagent control is performed to account for imperfect digestion by the RNase R enzyme. Once the

RNA modification reaction is complete, EDTA is added to chelate free Mg^{2+} and the RNA is recovered by ethanol precipitation to remove buffer components that may inhibit RNase R activity.

RNase R digestion

Sites of 2′-*O*-adduct formation are detected by *M. genitalium* RNase R[23], a 3′→5′ exoribonuclease that (i) is readily heat inactivated[6], (ii) degrades highly structured RNAs, and (iii) is inhibited by 2′-*O*-adducts in the substrate RNA. The enzyme is sensitive to Mg^{2+} concentration so it is critical that Mg^{2+} not be carried over from the chemical modification step. The RNase R enzyme is inactivated by addition of EDTA and heating at 95 °C for 3 min. A no reagent, no enzyme control is performed to identify intrinsic or pre-existing degradation sites in the RNA. The RNA fragments are then recovered by ethanol/isopropanol precipitation, optimized for recovery of small RNA fragments, and resolved by denaturing polyacrylamide gel electrophoresis.

Sequencing

A sequencing lane is used to assign the bands in the (+) and (−) SHAPE reagent lanes. Sequencing lanes are conveniently generated by kethoxal modification of denatured RNA followed by RNase R degradation of the RNA. Kethoxal covalently modifies single-stranded guanosine residues at the N1 and N2 positions to form a cyclic adduct[18]. SHAPE modification and kethoxal sequencing reactions can be performed concurrently. Kethoxal-mediated sequencing is advantageous because the resulting RNA fragments possess covalent adducts and 3′-ends that are similar to RNase-detected SHAPE fragments. For fragments longer than approximately 15 nucleotides, RNAs containing SHAPE and kethoxal adducts migrate essentially identically. There are small differences, approximately one-half of a nucleotide, in electrophoretic migration for shorter fragments. In practice, band assignment using kethoxal sequencing ladders is straightforward.

Data analysis and assignment of reactivities

RNase-detected SHAPE yields RNA fragments that terminate three nucleotides 3′ of the site of modification (Figure 2, inset). Kethoxal sequencing, detected by RNase R degradation, yields RNA fragments that terminate four nucleotides 3′ of the kethoxal-modified guanosine nucleotide. Thus, as visualized using 5′-labeled RNA, the kethoxal-mediated guanosine sequencing lanes are exactly one nucleotide shorter than the corresponding 2′-SHAPE adducts (Figure 3a). Band intensities, resolved on sequencing gels, can be conveniently quantified using the Semi-Automated Footprinting Analysis (SAFA) software[34]. SHAPE data are highly reproducible, differences in normalized reactivities between independent replicates are typically less than ±10% and 0.2 absolute SHAPE units.

MATERIALS

REAGENTS

- 5′-[^{32}P]-labeled RNA at a concentration of 0.1 μM or greater in 10 mM HEPES, pH 8.0

CRITICAL: RNA preparation must be performed in an RNase-free environment. RNA for modification and RNase R digestion can be stored in aliquots to reduce RNase contamination.

- Glycogen, 20 mg/mL (Roche, cat. no. 901393)
- EDTA, 0.5 M (Ambion, cat. no. 9260G)
- Formamide (Acros Organics, cat. no. AC18109)
- DMSO, molecular biology grade (Sigma-Aldrich, cat. no. 115959)

CRITICAL: DMSO bottle should be stored in a desiccator at room temperature.

- 1-methyl-7-nitroisatoic anhydride (1M7) (synthesis is described in ref. 12 and in a Supporting Protocol)

CRITICAL: 1M7 should be stored in a desiccator at 4 °C.

- Kethoxal (USB, cat. no. 17930)

CRITICAL: Kethoxal should be stored at −20 °C.

- *M. genitalium* RNase R, 4.5 mg/mL, conveniently obtained by affinity purification using a C-terminal $(His)_6$-tagged expression construct (see Supporting Protocol)
- Thiamine pyrophosphate (TPP) (Sigma-Aldrich, cat. no. C8754)
- Boric acid (Sigma-Aldrich, cat. no. B7901)
- SUPERase-In (Ambion, cat. no. AM2694)
- Alkaline phosphatase (Roche, cat. no. 1097075)
- T4 polynucleotide kinase (PNK) (New England Biolabs, cat. no. M0201S)
- 10× PNK buffer (New England Biolabs, cat. no. M0201S)
- γ-[^{32}P]-ATP (6×10^6 Ci/mol, 10 Ci/L, Perkin Elmer, cat. no. BLU502Z)
- Reagents for high-resolution polyacrylamide gel electrophoresis, including 29:1 acrylamide:bisacrylamide, 7 M urea, 1×TBE

REAGENT SETUP

RNase R stop dye (96% formamide, 1 mM EDTA, pH 8.0, containing bromophenol blue and xylene cyanol tracking dyes)

TE (10 mM Tris, 1 mM EDTA, pH 8.0)

3.3× RNA folding solution (333 mM HEPES, pH 8.0, 333 mM NaCl, 33 mM $MgCl_2$). A wide variety of solution conditions that stabilize the desired structural state of the RNA can be used. Buffer components, ionic strength, and ions can all be varied with the proviso that the pH should be maintained in the 7.6–8.3 range. In the SHAPE modification reaction, the buffer concentration should be greater than the final reagent concentration.

10× 1M7 in DMSO A good starting 10× 1M7 concentration is 80 mM. The useful range of 10× 1M7 concentration is 15–100 mM. Lower concentrations yield longer read lengths, but less intense bands.

10× kethoxal in H_2O A good starting 10× kethoxal concentration is 20 mM [equal to 1 μL neat kethoxal (7.88 M) in 393 μL H_2O].

10× RNase R reaction buffer (200 mM Tris-HCl, pH 8.0, 1 M KCl, 2.5 mM $MgCl_2$)

10× Thiamine pyrophosphate solution (50 μM)

5′-[^{32}P]-labeled RNA Prepared by performing the following steps: (i) Dephosphorylation reaction. Mix 50 mM Tris (pH 8.5), 0.1 mM EDTA, 50 pmol RNA, 300 units SUPERase-In, 200 units alkaline phosphatase in 300 μL. Incubate at 50 °C for 1 h. (ii) Phenol:chloroform:isoamyl alcohol extraction, ethanol precipitation, and resuspension in TE. (iii) 5′-End labeling. Mix 10 pmol dephosphorylated RNA, 70 mM Tris (pH 7.6), 10 mM $MgCl_2$, 5 mM DTT, 1 μL [γ-^{32}P]-ATP, 2 μL T4 polynucleotide kinase in 20 μL. Incubate at 37 °C for 30 min. (iv) Purify on 8% denaturing polyacrylamide gel (1× TBE, 7 M urea). Use autoradiography to visualize and excise the band corresponding to the radiolabeled RNA. (v) Passively elute RNA overnight into TE and remove acrylamide pieces using a centrifugal filter device. (vi) Recover radiolabeled RNA by ethanol precipitation (no glycogen should be used if RNA will be stored after radiolabeling). Resuspend pellet in 10 mM HEPES, pH 8.0. Alternatively, 5′-fluorescently labeled RNAs can be used, for labeling protocols see Refs. 30–31.

EQUIPMENT

- Amicon micropure-EZ centrifugal filter devices (Millipore, cat no. 42533)
- −20 °C freezer
- Microcentrifuge for 1.5 mL tubes at 4 °C
- Phosphorimaging instrument and screen
- Gel dryer
- Sequencing apparatus for high-resolution polyacrylamide gel electrophoresis. We use vertical denaturing gels of dimensions 0.75 mm (length) × 31 cm (width) × 38.5 cm (height) that are 10–12 % (29:1) acrylamide, 90 mM Tris-borate, 2 mM EDTA and 7 M urea.
- Programmable incubator or heat block

PROCEDURE

RNA folding TIMING 40 min

1. Add 0.4 pmol (~10,000 cpm) 5′-[^{32}P]-labeled RNA in 24 μL sterile H_2O to a 0.65 mL reaction tube.
2. Heat the RNA to 95 °C for 2 min; then immediately place on ice for 2 min.

3 Add 12 μL 3.3× folding solution and mix.

4 Incubate the tube at the desired reaction temperature (25 or 37 °C) for 10 min.

5 Preincubate a 0.65 mL reaction tube containing 2 μL 10× ligand solution (thiamine pyrophosphate) or H_2O.

6 Add 18 μL pre-folded RNA to 2 μL 10× ligand solution (thiamine pyrophosphate) or H_2O (in this example, the TPP riboswitch is probed in the ligand-free and ligand-bound states).

7 Incubate tube at the desired reaction temperature (25 or 37 °C) for 20 min.

RNA structure modification TIMING 1.5 h

8 Aliquot 1 μL 10× 1M7 in DMSO [for the (+) 1M7 reaction] and 1 μL neat DMSO [for the (−) 1M7 reaction (control)] into 0.65 mL reaction tubes.

9 Remove 9 μL of folded RNA and add to (+) and (−) 1M7 reactions. Mix thoroughly and incubate the reaction at 37 °C for 1.25 min. This is equivalent to five 1M7 hydrolysis half-lives[12].

? TROUBLESHOOTING

10 After the reaction has gone to completion, recover the RNA by ethanol precipitation. To each tube (4 total), add 2.5 μL 100 mM EDTA (to chelate Mg^{2+}), 90 μL sterile H_2O, 5 μL 4 M NaCl, 1 μL 20 mg/mL glycogen, 380 μL 100% ethanol; mix; and then incubate at −20 °C for 30 min. Precipitate the RNA by spinning at maximum speed (14000 rpm) in a microcentrifuge at 4 °C for 30 min.

? TROUBLESHOOTING

11 Remove ethanol supernatant and resuspend each RNA sample in 8 μL sterile H_2O.

CRITICAL: The activity of *M. genitalium* RNase R is very sensitive to Mg^{2+} concentration. It is essential to remove all Mg^{2+} from the RNA modification (structure probing) step prior to the RNase R detection step.

PAUSE POINT. The modified RNA can be stored at −20 °C overnight.

Kethoxal modification (performed concurrently with 1M7 modification)

12 Add 0.1 pmol 5′-[^{32}P]-labeled RNA in 16 μL sterile H_2O to a 0.65 mL reaction tube.

13 Heat the RNA to 95 °C for 2 min; then immediately place on ice for 2 min.

14 Add 2 μL 1 M HEPES (pH 8.0) and mix thoroughly.

15 Incubate the tube at 70 °C for 3 min.

16 Preincubate a 0.65 mL reaction tube containing 2 μL 20 mM kethoxal in sterile H_2O at 70 °C for 1 min.

17 Add the RNA to the kethoxal solution and mix well.

18 Incubate at 70 °C for 5 min.

? TROUBLESHOOTING

19 Quench reaction with 20 μL of 10 mM unbuffered boric acid.

20 Recover the RNA by ethanol precipitation. Add 60 μL sterile H_2O, 10 μL 4 M NaCl, 1 μL 20 mg/mL glycogen, 380 μL 100% ethanol; mix; then incubate at −20 °C for 30 min. Precipitate the RNA by spinning at maximum speed in a microcentrifuge at 4 °C for 30 min.

21 Remove ethanol supernatant and add 400 μL 70% ethanol. Invert the tube to dislodge and wash pellet. Recover RNA by spinning at maximum speed in a microcentrifuge at 4 °C for 2 min.

22 Repeat step 21.

23 Resuspend RNA in 8 μL sterile H_2O.

PAUSE POINT. The modified RNA can be stored at −20 °C overnight.

RNase R digestion TIMING 2 h

24 Add 1 μL 10× RNase R reaction buffer to RNAs from steps 11 and 23.

25 Add 1 μL *M. genitalium* RNase R (4.5 mg/mL) to each tube. Mix well.

CRITICAL: Use aerosol-resistant tips for all steps involving pipetting active RNase R and solutions containing this enzyme prior to the heat inactivation step.

26 Incubate tubes at 50 °C for 30 min.

CRITICAL: RNA secondary structure is destabilized at elevated temperatures which facilitates RNase R degradation of structured RNAs[6,35].

? TROUBLESHOOTING

27 Add 1 μL 100 mM EDTA then incubate at 95 °C for 3 min to inactivate RNase R.

CRITICAL: RNase R is irreversibly inactivated by heat[6]. This inactivation step is especially important to prevent RNase contamination when working in an RNA lab.

28 Recover RNA fragments by ethanol/isopropanol precipitation. To each tube add 90 μL sterile H_2O, 10 μL 4 M NaCl, 100 μL 100% isopropanol, 250 μL 100% ethanol; mix; and incubate at −20 °C for 30 min. Precipitate the RNA by spinning at maximum speed in a microcentrifuge at 4 °C for 45 min. (Alternatively, samples can be loaded directly onto the gel without ethanol/isopropanol precipitation. However, precipitation reduces the total volume, concentrates the intensity of the 5′-label, and removes salt and buffer components to yield improved gel resolution).

CRITICAL: Isopropanol is required to efficiently precipitate smaller RNA fragments. Omitting this step leads to loss of RNA fragments shorter than ~15 nucleotides.

? TROUBLESHOOTING

29 Remove supernatant and resuspend pellet in 7–9 μL RNase R stop dye.

30 Heat at 95 °C for 3 min.

PAUSE POINT. Samples can be stored at −20 °C overnight.

RNA fragment analysis by gel electrophoresis TIMING ~7 h

31 Load ~2 μL of each reaction (~5000 cpm) in individual lanes of a 10% polyacrylamide sequencing gel (29:1 acrylamide:bisacrylamide, 1× TBE, 7 M urea). To resolve both the 5′ and 3′ ends of the RNA, perform electrophoresis for 90 min at 70 W, then reload the same samples in unoccupied lanes on the gel and continue electrophoresis for 150 min at 70 W. The samples loaded first will have been subjected to electrophoresis for ~240 min which will resolve nucleotides close to the 3′ end of the RNA; whereas, samples loaded later will provide data on the 5′ region.

? TROUBLESHOOTING

32 Dry the gel using a heated vacuum gel dryer for ~1 h.

? TROUBLESHOOTING

33 Expose the gel overnight to a phosphor screen and quantify scanned bands using a phosphorimaging instrument. Quantify the intensity of every well-defined band in the gel for the (+) and (−) 1M7 lanes by two-dimensional densitometry using SAFA[34].

34 Calculate the absolute SHAPE reactivity at each position in the RNA by subtracting the (−) 1M7 intensities from the (+) 1M7 intensities. In general, the data are normalized by excluding the top 2% of the reactive nucleotides, averaging the next 10% of reactive nucleotides, and then dividing all intensities by this averaged value[22] (Supplemental Dataset 1). For longer RNAs, it may be necessary to correct for signal decay, as described[7,13]. The guanosine sequencing lanes generated by RNase R-detected kethoxal modification are exactly one nucleotide shorter than the corresponding sites of 1M7 modification.

TIMING

Steps 1–7: 40 min

Steps 8–11 and 12–23: 1.5 h

Steps 24–30: 2 h

Step 31: ~ 4 h

Steps 32–34: 3 h plus time necessary to expose screen

TROUBLESHOOTING

Troubleshooting advice can be found in Table 1.

ANTICIPATED RESULTS

RNase-detected SHAPE makes possible single nucleotide analysis of local nucleotide flexibility for most nucleotides in an RNA, including those at the 5′ and 3′ ends. The experiment is performed in a single reaction tube and yields direct and experimentally straightforward detection of RNA covalent adducts.

The representative experiment described here was performed using an 80 nucleotide *in vitro* transcript corresponding to the aptamer domain of the thiamine pyrophosphate-sensing (TPP) riboswitch from the *E. coli thiM* mRNA[36]; no flanking sequences were added. The TPP RNA structure was probed in both the ligand-free and ligand-bound states. Kethoxal-mediated sequencing at guanosine nucleotides were used to assign bands observed in the (+) and (−) SHAPE reagent lanes (Figure 3a). Bands at the top of the gel correspond to undigested full-length RNA and larger RNA fragments that are not fully resolved in this particular electrophoresis run (Figure 3a). Bright bands at the bottom of the gel are short oligonucleotide fragments that reflect the short RNA “handle” by which RNase R binds RNA, and correspond to the end products of 3′→5′ exoribonuclease digestion. Using RNase R-detected SHAPE, we resolved and quantified SHAPE reactivities for both the ligand-free and the ligand-bound riboswitch RNA states (Figure 3b).

RNase-detected SHAPE accurately recapitulates the previously characterized base-pairing pattern and tertiary structure interactions of the TPP-bound state[36]. Regions that are directly involved in TPP binding (J3-2 and nts 60–61, Figures 3b, 4b, 4c) are constrained and unreactive in the ligand-bound state. The prominent long-range tertiary interaction involving the L5 loop binding to the P3 helix results in low SHAPE reactivities for the loop nucleotides (Figures 3b and 4b).

RNase-detected SHAPE also revealed that the riboswitch aptamer domain undergoes significant conformational changes upon TPP binding as previously reported[6] [compare (−) and (+) TPP reactions, Figure 3]. The SHAPE data support a specific, nucleotide resolution, secondary structure model for the ligand-free state[6]. The ligand-free state forms an open Y-conformation in which unreactive helices (P2–P5) are linked together by relatively reactive and thus conformationally flexible joining regions (J2-4, J3-2 and nucleotides 60–62) (Figure 4a).

Comparing the SHAPE-supported ligand-free and ligand-bound states reveal changes that are consistent with previously described large-scale structural changes associated with ligand binding[36–38] (see J3-2 and nts 60–61, Figure 4). In addition to these changes, RNase-detected SHAPE uniquely reveals important fine-scale changes. For example, SHAPE detects formation of the A53-A84 non-canonical base-pair in the ligand-bound state (Figure 4). Also, RNase-detected SHAPE reveals a single nucleotide register shift in the P3 helix upon ligand binding. In the ligand-free state, C22 is reactive and likely to be a single-stranded bulge; whereas, in the ligand-bound state, C24 is reactive while C22 is unreactive.

Thus, C24 forms a bulged structure in the TPP-bound state (Figure 4). This register shift likely plays an important structural role because C24 mediates a stacking interaction with A69[36,38], a nucleotide that contributes to docking of the loop nucleotides in L5 with the P3 helix.

Superposition of SHAPE reactivities on the three-dimensional structure for the TPP-bound RNA riboswitch domain emphasizes the tight packing of this RNA. Although this RNA contains numerous regions that are depicted as single stranded in a secondary structure diagram, many of these elements are constrained by non-canonical local interactions or interactions with the TPP ligand and are unreactive (Figure 4c, nucleotides in black). The core of the TPP riboswitch aptamer domain is tightly packed and highly constrained. Locally flexible nucleotides, as measured by SHAPE, lie almost exclusively at the exterior of the structure (Figure 4c, emphasized in orange and red).

RNase-detected SHAPE allows quantitative, single-nucleotide detection of covalent adducts at the 2′-OH position and at base-pairing faces of the nucleobases using an adduct-inhibited 3′→5′ exoribonuclease, RNase R. RNase R-mediated detection is simple to implement and should be broadly applicable for detection of diverse classes of covalent adducts in RNA. RNase-detected SHAPE will allow for direct single-nucleotide structural analysis of previously inaccessible RNAs, especially short non-coding RNAs and RNAs with functionally important structures at their 5′ and 3′ ends.

Supplementary Material

Refer to Web version on PubMed Central for supplementary material.

Acknowledgments

We are indebted to Arun Malhotra for many productive discussions regarding the mechanism of RNase R enzymes and to Zhongwei Li for the gift of a plasmid encoding *M. genitalium* RNase R optimized for expression in *E. coli*. We thank Philip Homan for helpful discussions regarding synthesis of 1M7. This work was supported by a grant from the National Science Foundation (MCB-0919666 to KMW); NAS is a Fellow of the UNC Lineberger Comprehensive Cancer Center.

References

1. Gesteland, RF.; Cech, TR.; Atkins, JF. The RNA World. Cold Spring Harbor Laboratory Press; Cold Spring Harbor, New York: 2004.
2. Li PT, Vieregg J, Tinoco I Jr. How RNA unfolds and refolds. Annu Rev Biochem. 2008; 77:77–100. [PubMed: 18518818]
3. Brunel C, Romby P. Probing RNA structure and RNA-ligand complexes with chemical probes. Methods Enzymol. 2000; 318:3–21. [PubMed: 10889976]
4. Weeks KM. Advances in RNA structure analysis by chemical probing. Curr Opin Struct Biol. 2010; 20:295–304. [PubMed: 20447823]
5. Wilkinson KA, Merino EJ, Weeks KM. RNA SHAPE chemistry reveals nonhierarchical interactions dominate equilibrium structural transitions in tRNA(Asp) transcripts. J Am Chem Soc. 2005; 127:4659–67. [PubMed: 15796531]
6. Steen KA, Malhotra A, Weeks KM. Selective 2′-hydroxyl acylation analyzed by protection from exoribonuclease. J Am Chem Soc. 2010; 132:9940–3. [PubMed: 20597503]

7. Wilkinson KA, Gorelick RJ, Vasa SM, Guex N, Rein A, Mathews DH, Giddings MC, Weeks KM. High-throughput SHAPE analysis reveals structures in HIV-1 genomic RNA strongly conserved across distinct biological states. PLoS Biol. 2008; 6:e96. [PubMed: 18447581]
8. Watts JM, Dang KK, Gorelick RJ, Leonard CW, Bess JW Jr, Swanstrom R, Burch CL, Weeks KM. Architecture and secondary structure of an entire HIV-1 RNA genome. Nature. 2009; 460:711–6. [PubMed: 19661910]
9. Merino EJ, Wilkinson KA, Coughlan JL, Weeks KM. RNA structure analysis at single nucleotide resolution by selective 2′-hydroxyl acylation and primer extension (SHAPE). J Am Chem Soc. 2005; 127:4223–31. [PubMed: 15783204]
10. Wilkinson KA, Vasa SM, Deigan KE, Mortimer SA, Giddings MC, Weeks KM. Influence of nucleotide identity on ribose 2′-hydroxyl reactivity in RNA. RNA. 2009; 15:1314–21. [PubMed: 19458034]
11. Gherghe CM, Shajani Z, Wilkinson KA, Varani G, Weeks KM. Strong correlation between SHAPE chemistry and the generalized NMR order parameter (S^2) in RNA. J Am Chem Soc. 2008; 130:12244–5. [PubMed: 18710236]
12. Mortimer SA, Weeks KM. A fast-acting reagent for accurate analysis of RNA secondary and tertiary structure by SHAPE chemistry. J Am Chem Soc. 2007; 129:4144–5. [PubMed: 17367143]
13. Badorrek CS, Weeks KM. Architecture of a gamma retroviral genomic RNA dimer. Biochemistry. 2006; 45:12664–72. [PubMed: 17042483]
14. Duncan CD, Weeks KM. Nonhierarchical ribonucleoprotein assembly suggests a strain-propagation model for protein-facilitated RNA folding. Biochemistry. 2010; 49:5418–25. [PubMed: 20533823]
15. Wang B, Wilkinson KA, Weeks KM. Complex ligand-induced conformational changes in tRNA(Asp) revealed by single-nucleotide resolution SHAPE chemistry. Biochemistry. 2008; 47:3454–61. [PubMed: 18290632]
16. Gherghe C, Lombo T, Leonard CW, Datta SA, Bess JW Jr, Gorelick RJ, Rein A, Weeks KM. Definition of a high-affinity Gag recognition structure mediating packaging of a retroviral RNA genome. Proc Natl Acad Sci U S A. 2010; 107:19248–53. [PubMed: 20974908]
17. Deigan KE, Li TW, Mathews DH, Weeks KM. Accurate SHAPE-directed RNA structure determination. Proc Natl Acad Sci U S A. 2009; 106:97–102. [PubMed: 19109441]
18. Ehresmann C, Baudin F, Mougel M, Romby P, Ebel JP, Ehresmann B. Probing the structure of RNAs in solution. Nucleic Acids Res. 1987; 15:9109–28. [PubMed: 2446263]
19. Stern S, Moazed D, Noller HF. Structural analysis of RNA using chemical and enzymatic probing monitored by primer extension. Methods Enzymol. 1988; 164:481–9. [PubMed: 2468070]
20. Mitra S, Shcherbakova IV, Altman RB, Brenowitz M, Laederach A. High-throughput single-nucleotide structural mapping by capillary automated footprinting analysis. Nucleic Acids Res. 2008; 36:e63. [PubMed: 18477638]
21. McGinnis JL, Duncan CD, Weeks KM. High-throughput SHAPE and hydroxyl radical analysis of RNA structure and ribonucleoprotein assembly. Methods Enzymol. 2009; 468:67–89. [PubMed: 20946765]
22. Wilkinson KA, Merino EJ, Weeks KM. Selective 2′-hydroxyl acylation analyzed by primer extension (SHAPE): quantitative RNA structure analysis at single nucleotide resolution. Nat Protoc. 2006; 1:1610–6. [PubMed: 17406453]
23. Lalonde MS, Zuo Y, Zhang J, Gong X, Wu S, Malhotra A, Li Z. Exoribonuclease R in Mycoplasma genitalium can carry out both RNA processing and degradative functions and is sensitive to RNA ribose methylation. RNA. 2007; 13:1957–68. [PubMed: 17872508]
24. Vincent HA, Deutscher MP. The roles of individual domains of RNase R in substrate binding and exoribonuclease activity. The nuclease domain is sufficient for digestion of structured RNA. J Biol Chem. 2009; 284:486–94. [PubMed: 19004832]
25. Matos RG, Barbas A, Arraiano CM. RNase R mutants elucidate the catalysis of structured RNA: RNA-binding domains select the RNAs targeted for degradation. Biochem J. 2009; 423:291–301. [PubMed: 19630750]

26. Frazao C, McVey CE, Amblar M, Barbas A, Vonrhein C, Arraiano CM, Carrondo MA. Unravelling the dynamics of RNA degradation by ribonuclease II and its RNA-bound complex. Nature. 2006; 443:110–4. [PubMed: 16957732]
27. Lorentzen E, Basquin J, Tomecki R, Dziembowski A, Conti E. Structure of the active subunit of the yeast exosome core, Rrp44: diverse modes of substrate recruitment in the RNase II nuclease family. Mol Cell. 2008; 29:717–28. [PubMed: 18374646]
28. Barbas A, Matos RG, Amblar M, Lopez-Vinas E, Gomez-Puertas P, Arraiano CM. Determination of key residues for catalysis and RNA cleavage specificity: one mutation turns RNase II into a "SUPER-ENZYME". J Biol Chem. 2009; 284:20486–98. [PubMed: 19458082]
29. Mortimer SA, Weeks KM. Time-resolved RNA SHAPE chemistry. J Am Chem Soc. 2008; 130:16178–80. [PubMed: 18998638]
30. Qin PZ, Pyle AM. Site-specific labeling of RNA with fluorophores and other structural probes. Methods. 1999; 18:60–70. [PubMed: 10208817]
31. Bakin AV, Borisova OF, Shatsky IN, Bogdanov AA. Spatial organization of template polynucleotides on the ribosome determined by fluorescence methods. J Mol Biol. 1991; 221:441–53. [PubMed: 1717698]
32. Gherghe CM, Mortimer SA, Krahn JM, Thompson NL, Weeks KM. Slow conformational dynamics at C2′-endo nucleotides in RNA. J Am Chem Soc. 2008; 130:8884–5. [PubMed: 18558680]
33. Weeks KM, Mauger DM. Exploring RNA structural codes with SHAPE chemistry. Acc Chem Res. 2011; 44 in press.
34. Das R, Laederach A, Pearlman SM, Herschlag D, Altman RB. SAFA: semi-automated footprinting analysis software for high-throughput quantification of nucleic acid footprinting experiments. RNA. 2005; 11:344–54. [PubMed: 15701734]
35. Vincent HA, Deutscher MP. Insights into how RNase R degrades structured RNA: analysis of the nuclease domain. J Mol Biol. 2009; 387:570–83. [PubMed: 19361424]
36. Serganov A, Polonskaia A, Phan AT, Breaker RR, Patel DJ. Structural basis for gene regulation by a thiamine pyrophosphate-sensing riboswitch. Nature. 2006; 441:1167–71. [PubMed: 16728979]
37. Lang K, Rieder R, Micura R. Ligand-induced folding of the thiM TPP riboswitch investigated by a structure-based fluorescence spectroscopic approach. Nucleic Acids Res. 2007; 35:5370–8. [PubMed: 17693433]
38. Kulshina N, Edwards TE, Ferre-D'Amare AR. Thermodynamic analysis of ligand binding and ligand binding-induced tertiary structure formation by the thiamine pyrophosphate riboswitch. RNA. 2010; 16:186–96. [PubMed: 19948769]
39. Zhang Y. I-TASSER server for protein 3D structure prediction. BMC Bioinformatics. 2008; 9:40. [PubMed: 18215316]

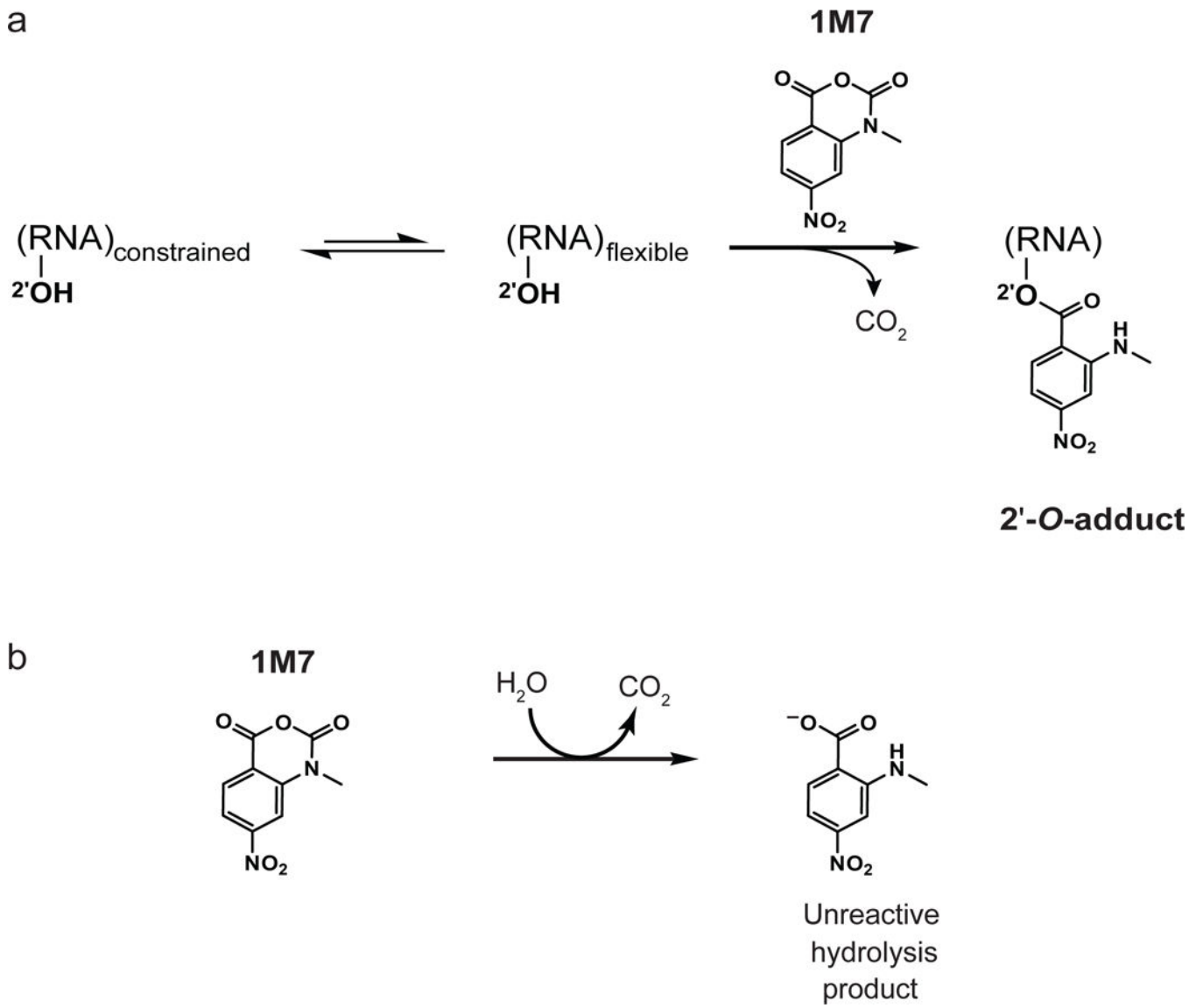

Figure 1.

RNA SHAPE chemistry. (**a**) SHAPE reagents, including 1M7, react preferentially at conformationally flexible nucleotides to form 2′-*O*-adducts. (**b**) Concurrent reagent auto-inactivation by hydrolysis.

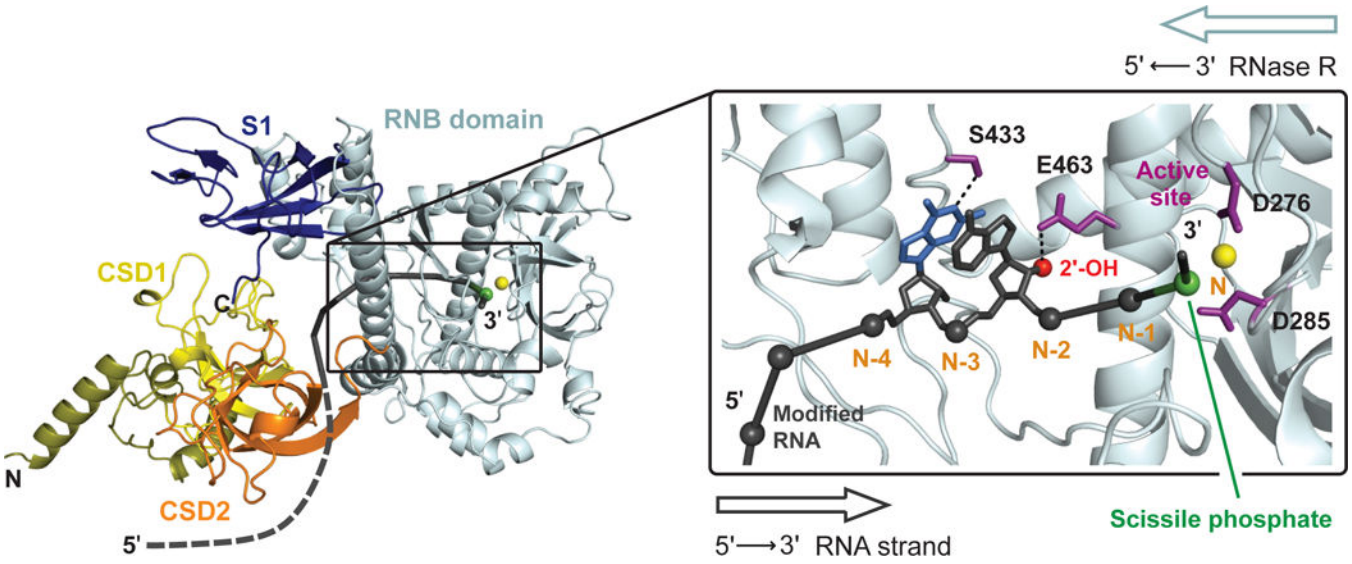

Figure 2.

Model of *Mycoplasma genitalium* RNase R and the interactions that mediate covalent adduct detection in RNA. The path of the RNA strand (in dark gray) is shown relative to the major enzyme domains. Inset illustrates the substrate-binding channel of the ribonuclease (RNB) domain. Modification of a 2′-hydroxyl group prevents exoribonuclease digestion; the modified residue is shown as a red sphere at N-3. The nucleobase whose base-pairing face is recognized by hydrogen bonding with serine 433 is shown in blue at N-4. The site of RNA strand hydrolysis is shown as a green sphere and a catalytic Mg^{2+} ion is yellow. The homology model was generated using I-TASSER[39]. Figure is adapted in part from ref. 6.

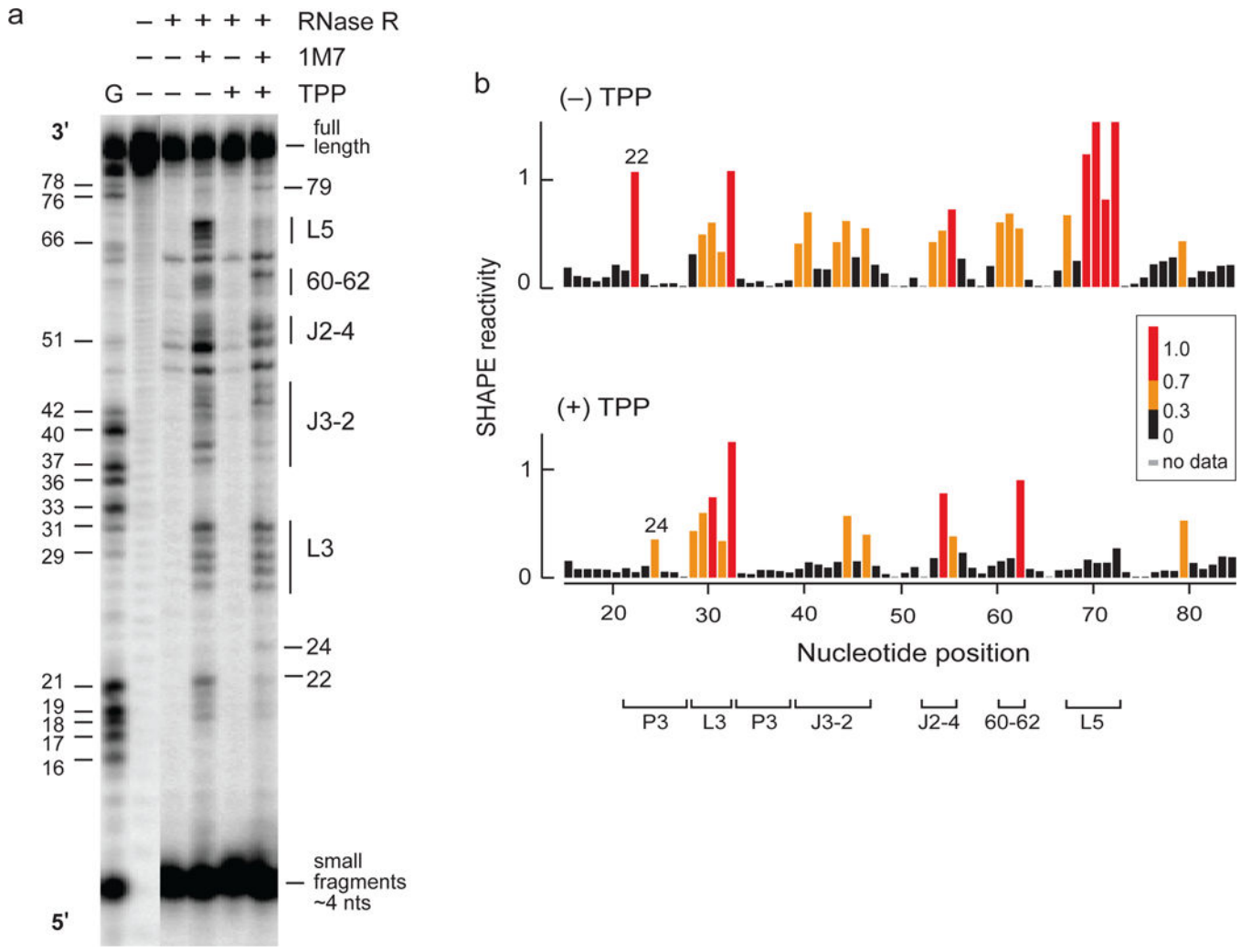

Figure 3.

Representative RNase-detected SHAPE experiment. (**a**) SHAPE reactions, performed using the 1M7 reagent, for the (80 nucleotide) TPP riboswitch domain and kethoxal-mediated sequencing (indicated with a G) resolved by denaturing polyacrylamide gel electrophoresis. The guanosine sequencing marker is one nucleotide shorter than bands corresponding to the (−) and (+) 1M7 reactions. Guanosine nucleotides are indicated at left; structural landmarks in the RNA are highlighted on the right. (**b**) Absolute SHAPE reactivities in the absence (top) and presence (bottom) of TPP ligand. Columns are colored by individual nucleotide SHAPE reactivities (see scale). SHAPE data are normalized to a scale in which zero indicates no reactivity and 1.0 is defined as the average intensity of highly reactive positions (step 34)[22].

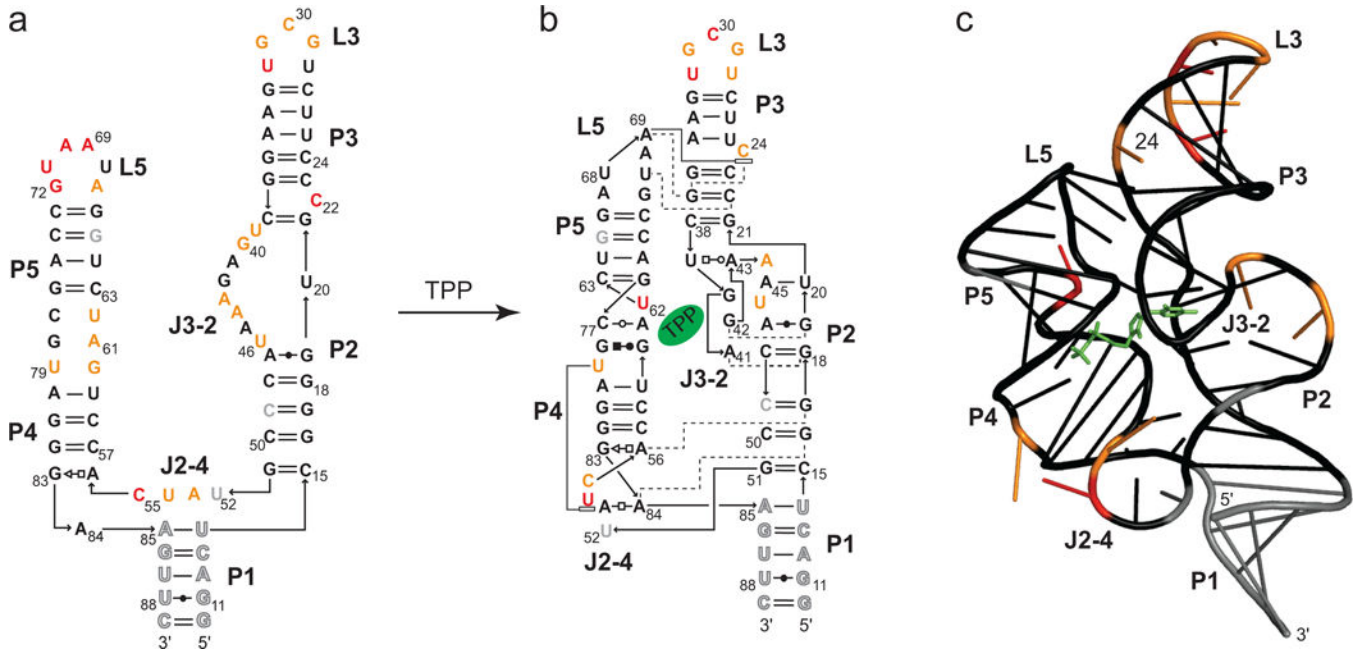

Figure 4.

Structural transitions in the TPP riboswitch aptamer domain visualized by RNase-detected SHAPE. Absolute SHAPE reactivities are superimposed on secondary structure models for the riboswitch RNA in the (**a**) absence and (**b**) presence of TPP ligand. (**c**) Tertiary structure[36] of the TPP-bound state. Nucleotides are colored by SHAPE reactivity using the scale shown in Figure 3. Nucleotides not probed in this experiment are shown in gray. Portions of this figure were reproduced with permission from ref. 6.

Table 1

Step	Problem	Reason	Solution
1–31	Bright bands present in the (−) 1M7 lane.	RNase contamination, most commonly caused by endonucleases.	Identify contaminated solution using an RNase detection kit or by evaluating each step of the protocol by resolving a labeled test RNA on a denaturing gel.
1–31	Low band intensities in all lanes.	5′-[^{32}P]-labeled RNA does not have sufficient specific activity. Not enough 5′-[^{32}P]-labeled RNA used for each experiment.	Repeat with freshly prepared [^{32}P]-labeled RNA. Repeat with a higher concentration of RNA.
6	Nucleotide transitions associated with ligand binding are not observed; (+) and (−) ligand states are identical.	Ligand binding is not occurring.	Increase ligand concentration.
8–9	Low or no signal in (+) 1M7 lane.	Insufficient modification of RNA.	Perform modification using a 2-fold higher concentration of 1M7. Ensure that 1M7 stock is kept dry – trace amounts of water will react with reagent. Make sure DMSO stock solution is also kept dry. Make fresh 1M7 solution for each experiment.
8–9	Bands observed close to the 3′ end of the RNA (top of gel), but no small RNA fragments observed.	Excessive modification of RNA.	Perform structure modification step using a 2-fold lower concentration of reagent.
10, 24–26	Very low signal in the (+) 1M7 lane and an intense full-length RNA band is observed.	Poor or inefficient RNase R digestion.	RNase R is very sensitive to Mg^{2+} concentration – ensure that final divalent ion concentration is 0.25 mM. Use desalting columns after modification. Use fresh stock of RNase R if enzyme activity is low. Increase enzyme concentration or digestion time.
15–18	Some guanosine residues are not detected in the kethoxal sequencing lane.	Complete kethoxal modification prevented by RNA folding.	Repeat kethoxal modification step at 90 °C to insure that RNA is denatured.
16–18	No sequencing bands in kethoxal lane.	Insufficient kethoxal modification of RNA.	Increase kethoxal concentration and/or reaction time. Make fresh kethoxal solution for each experiment.
24–26	Bright bands observed in (−) and (+) 1M7 lanes that do not correspond to modification stops or RNase contamination.	Structure-induced pausing by RNase R enzyme.	Heat RNA in sterile H_2O to 95 °C for 3 min, and place tube on ice. Add enzyme and incubate tube immediately at 50 °C. Increase digestion time.
28	No small oligonucleotide fragments in any lane.	Loss of small fragments during ethanol precipitation.	Add glycogen to ethanol/isopropanol precipitation step. Increase incubation time at −20 °C.
31	The faintest bands in the (+) 1M7 lane have significantly different intensities as compared to the corresponding bands in the (−) 1M7 lanes.	Random error involved with volume measurement; gel loaded unevenly.	Small differences in background intensity can be accounted for by statistical normalization (step 34). If intensities are significantly different, the gel should be re-run by loading samples with similar amounts of RNA in each lane.
31	Low resolution of bands in all lanes (smearing).	Overloading of gel lane. Uneven heating of gel during electrophoresis. Excess salt present in samples before loading on gel.	Reduce the volume or concentration of RNA loaded onto gel. Ensure that electrophoresis equipment works well. Perform additional 70% ethanol wash. Use desalting columns after RNase R digestion.
32		Gel drying is not effective.	Ensure that gel dryer seals properly.